INVESTIGATION ON DYNAMIC LOADS ON COUPLINGS OF HEAVY HIGH PRODUCTIVITY FREIGHT VEHICLLES

A. BUCKO
Senior Engineer at Smedley's Engineers and accredited PBS assessor in Australia. B.Sc, B. Eng.(Hons) at Monash University

D. SIMMS
Senior Engineer at Smedley's Engineers. B.Eng (Automotive) at RMIT University

A.BUCKERDIGE
Former Graduate Engineer at Smedley's Engineers
B. Eng.(Hons) and B.Math.
at University of Queensland

Abstract

This paper is an update to the progress of an on-road testing project to investigate and analyse the forces experienced by mechanical couplings in multi-combination vehicles and what factors contribute to the magnitude of these forces. The goal of the testing scheme is to address the suitability of the current D-rating equations outlined in AS2213.1 and AS4968.1 and extend the underlying dataset to include vehicles of a GCM of more than 125 tonnes.

Keywords: Heavy Vehicles, Mechanical Connections, Couplings, Pin type, 5th Wheel, Fifth Wheel, Road Train, AS2213, AS4968

1. Background

AS2213.1 and AS4968.1 are Australian Standards that govern the selection, marking, design, and performance requirements of mechanical connections between vehicles. Equations 1 and 2 below are the equations that dictate the minimum D-rating required for a coupling within a combination for pin type and fifth wheel respectively.

$$D = 0.6\frac{M_1 \times M_2}{M_1 + M_2} \times gravity \qquad (1)$$

$M_1 - Mass\ before\ the\ coupling$
$M_2 - Mass\ after\ the\ coupling$
$D - D\ rating\ value$

$$D = \frac{4.9T_4(R_4 + 0.08T_4)}{M - U} \qquad (2)$$

$R_4 - Mass\ after\ the\ coupling$
$T_4 - Mass\ before\ the\ coupling$
$M - GCM\ of\ Combination$
$U - Static\ vertical\ force\ onto\ 5th\ wheel$

As part of this coupling safety project which is funded by the National Heavy Vehicle Regulator's (NHVR) Heavy Vehicle Safety Initiative (HVSI), supported by the Australian Government, Smedley's Engineers were engaged to conduct an on-road testing scheme. The purpose was to gather real road loads on a high-GCM vehicle and determine which variables affect the forces seen in the couplings. Historic testing was conducted up to 125 t GCM due to the typical vehicles in operation at the time. Increases in vehicle safety systems, prime mover capability and an ongoing push for greater productivity have seen an increase in combination GCMs beyond that point.

There are several goals for the project, culminating in an ultimate outcome of determining whether the existing equations in use are suitable for D-rating selection for higher GCM vehicles.

Equations 1 and 2 assert that the forces acting upon the coupling are determined predominantly by the sum of the vehicle mass before and after the coupling, and as the coupling position approaches the centre of mass of the combination, the forces imposed upon the couplings should increase to a maximum. There is no limit inherent in these equations, so coupling forces are implied to increase perpetually as GCM increases.

The data logged during the testing regime will be analysed to determine whether the assertions of the equations are reflected in the road testing.

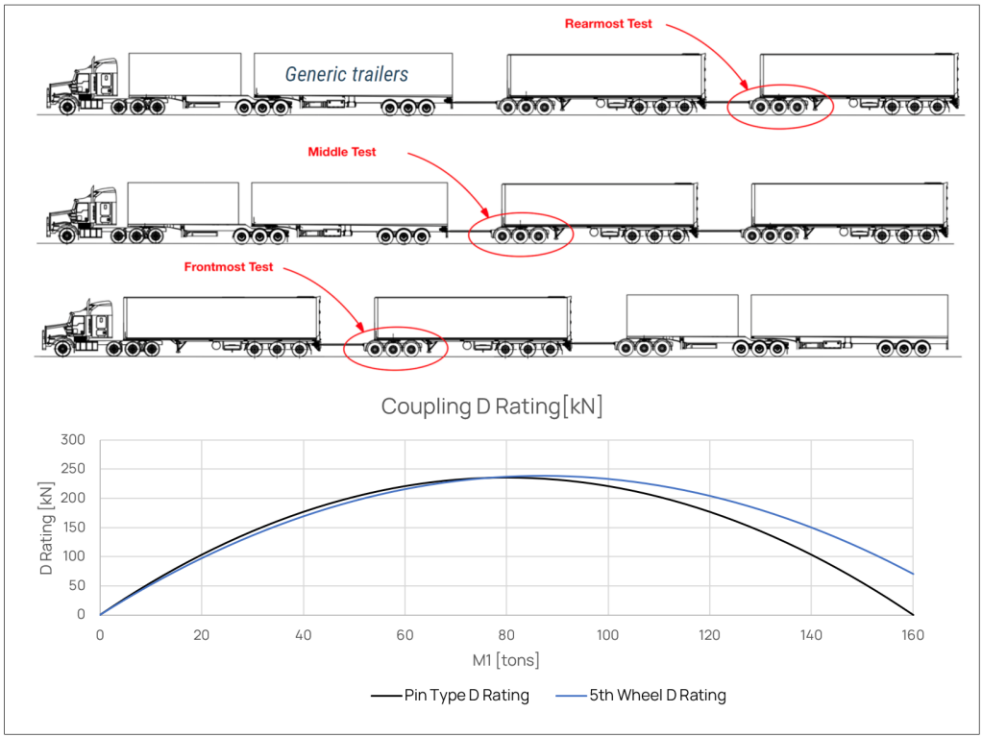

Figure 1 - Diagram showing the different configurations in the testing scheme, and the D-rating as a function of mass before the coupling (for a GCM of 160t) for pin type and fifth wheel type mechanical couplings

2. Testing Method

While designing the testing scheme, a range of factors were considered to decide how the test vehicle was to be setup. The considerations are listed below:

- Test at higher combination mass than previously tested, i.e. 125 t up to 160 t GCM, to determine if combination mass before/after is a primary variable in coupling forces.
- Test at different coupling positions along the combination, to understand the relationship between total combination mass and mass before/after.
- Test at the shortest possible drawbar length for the most aggressive arc, and investigate the relationship between speed, trailer relative vertical movement before/after, and forces.
- Test both on rough roads, and on roads where high speeds can be attained, to determine if the increased energy of road inputs with speed has a relationship to coupling forces.

Smedley's Engineers partnered with Direct Haul and Howard Porter to conduct the testing scheme. Direct Haul conduct fuel supply runs with road trains in the Northern Territory. Testing in the Northern Territory provided ready access to 160+ t GCM vehicles operating on public roads. Local advice was sought on routes containing a mixture of highway speeds and rough road features.

The test dolly, supplied by Howard Porter, was outfitted with an array of force, acceleration and road surface measurement instrumentation.

To ensure comprehensive data collection, the configuration of the road train was changed between consecutive runs to relocate the instrumented dolly, as shown in Figure 1. This allowed the reactions from the dolly to be recorded over the same sections of road for all three dolly positions.

The instrumentation used in the test included loadcells, accelerometers, ultrasonic distance sensors and GPS. The data logged from these sensors allowed the parameters of interested to be determined in post-processing. The list of these parameters is shown below.

- Longitudinal, Lateral & Vertical Pin Type Coupling Forces
- Longitudinal & Vertical Fifth Wheel Forces
- Fifth Wheel Overturning Moment
- Wheel Paths Vertical Profile
- Geospatial Position and Speed

2.1 Load Cells

Individual calibrated loadcells were used to measure the forces in this testing scheme. The load cells were developed in-house using full Wheatstone bridge strain gauges where the data was measured by an ADC and was transmitted onto a testing CANBUS network at a rate of 80 Hz.

Uncertainty about the source of a test dolly at that time, and the expected forces, pushed the authors towards manufacturing a modular solution of an M16 Grade 12.9 stud with load sensing that could be made to work in a range of locations. Prior testing in a similar smaller scale trial highlighted that direct strain gauging on the tow eye and fifth wheel feet has some limitations. Surface roughness, cross-sectional inconsistency and strain dead zones could all introduce unknown factors, which are solved using this modular method. Onboard digitisation of measurements was required to facilitate dangerous goods electrical compliance, IP56 equipment rating and fast reconfiguration of dolly position.

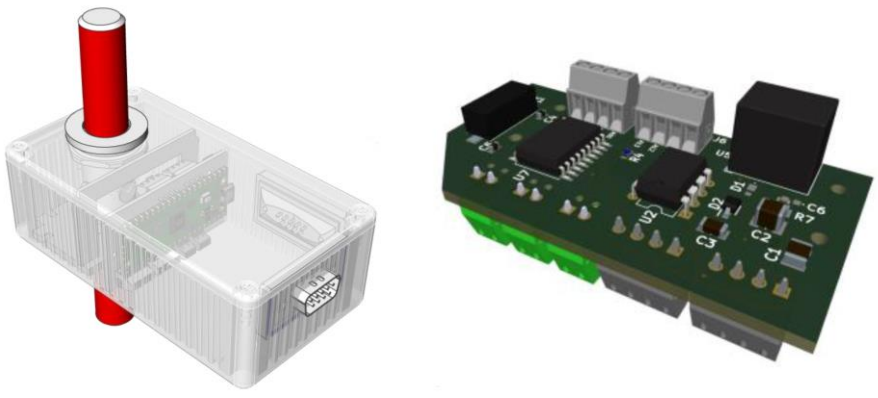

Figure 2 - Render of the load cells and the on-board digitiser

2.2 Drawbar Load Cells

The drawbar forces were measured by six loadcells in a flange, in line with the longitudinal load path. The total longitudinal force was calculated by summing the results from all the load cells. Lateral and vertical forces were also available, after calculating the summations of the moments, which are shown in the equations below.

$$F_{Longitudinal} = \sum^{i} F_{Loadcell_i}$$

$$F_{Lateral} = \frac{1}{L_{toweye}} \sum^{i} F_{Loadcell_i} \times y_i$$

$$F_{Vertical} = \frac{1}{L_{toweye}} \sum^{i} F_{Loadcell_i} \times z_i$$

$L = Distance\ from\ the\ centre\ of\ the\ toweye\ to\ the\ medial\ plane\ of\ the\ strain\ gauge$

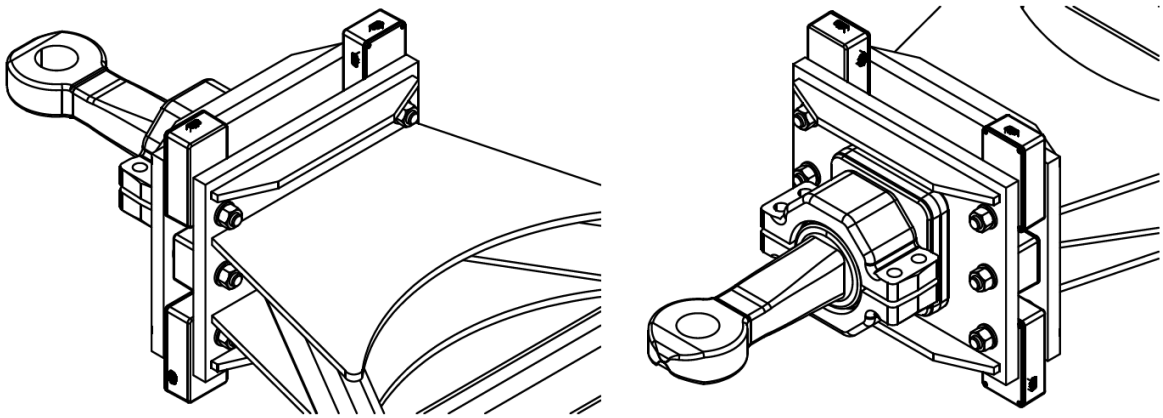

Figure 3 - Diagram of the drawbar showing the locations of the loadcells

2.2 Fifth Wheel Load Cells

The forces being transmitted through the fifth wheel were measured using 14 load cells that were in the load path. The location of each of these sensors was known so the longitudinal forces, overturning moment and vertical forces could be determined, which were calculated using the equations listed below.

$$F_{Longitudinal} = \frac{1}{L} \sum^{i} F_{Loadcell_i} \times x_i$$

$$M_{Overturning} = \frac{1}{L} \sum^{i} F_{Loadcell_i} \times y_i$$

$$F_{Vertical} = \sum^{i} F_{Loadcell_i}$$

$L = Moment\ arm\ from\ the\ medial\ plane\ of\ the\ strain\ gauge\ to\ fifth\ wheel\ pivot$

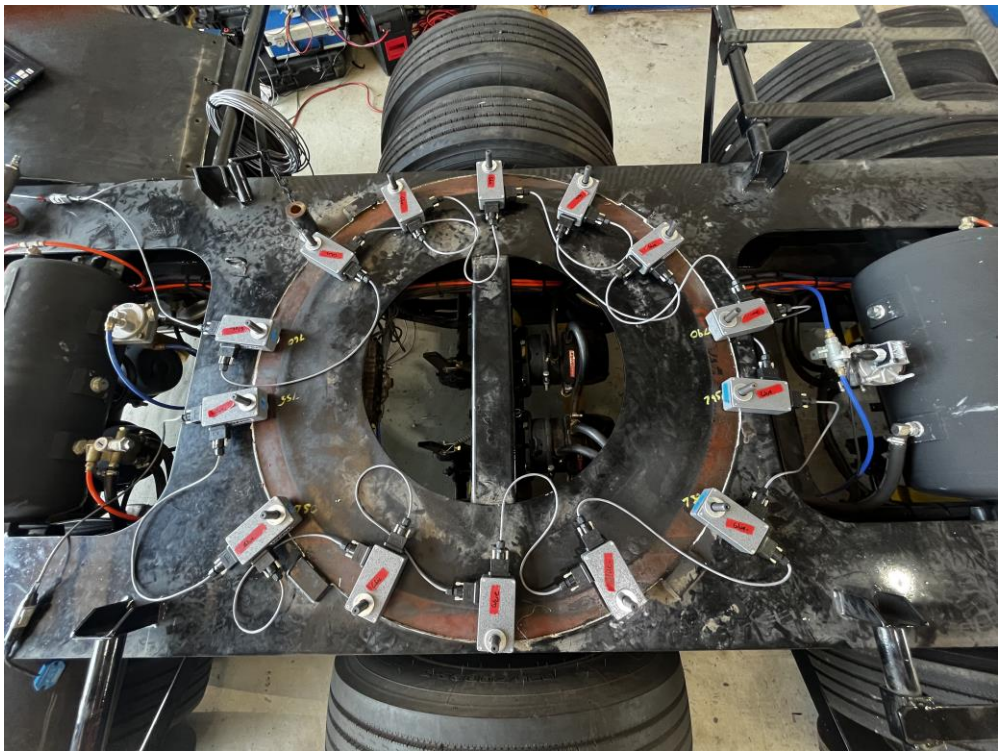

Figure 4 - Layout of the Fifth Wheel Load Sensors

2.3 Accelerometers

Three accelerometers were used during the testing scheme, the locations of these accelerometers are highlighted by the red symbols shown in Figure 5. The first accelerometer was mounted on the test dolly near the fifth wheel to determine the accelerations of the test dolly close to the fifth wheel. The second was mounted on the front of the test dolly, in line with the ultrasonic sensors, as a chassis movement compensation to inform wheel path measurements. The third accelerometer was positioned on the rear axle (unsprung) of the trailer in front of the test dolly.

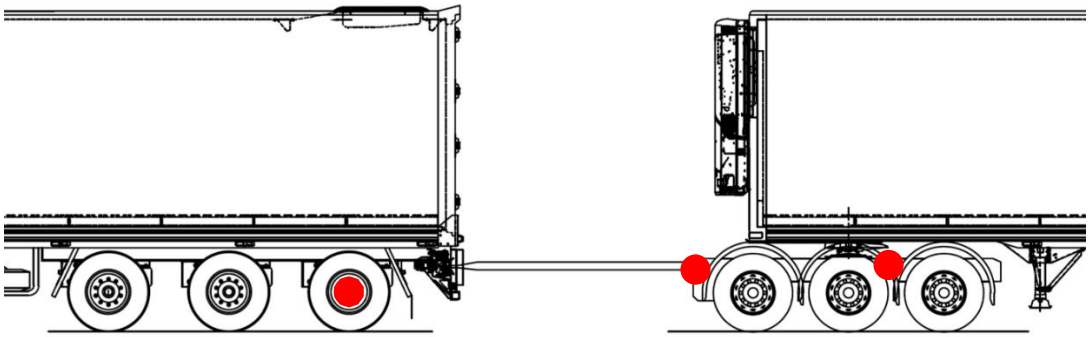

Figure 5 - Locations of the accelerometers

2.4 Ultrasonic sensors:

Three ultrasonic sensors were used to measure the distance to the ground at the centre of each wheel path and at the centre of the dolly. Measurement of the road surface allowed the vertical profile and crossfall of the road to be determined, after significant post processing.

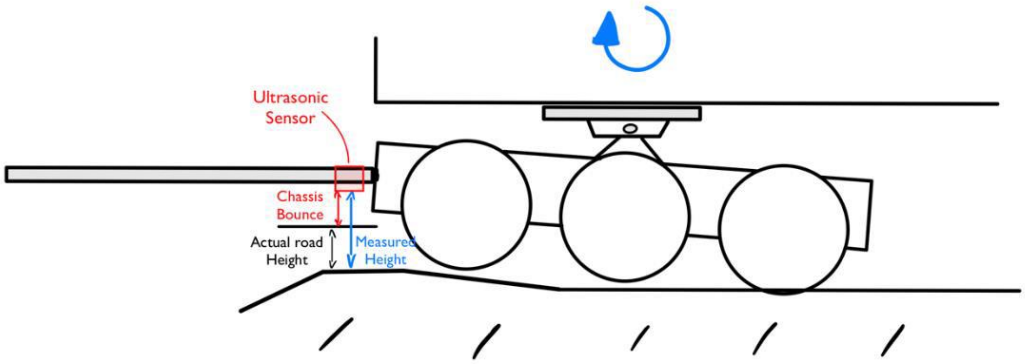

Figure 6 - Ultrasonic road profile measurement

3. Test Results and Analysis

3.1 Coupling Forces

Observed forces typically follow one of two patterns at both the pin type coupling and associated fifth wheel:

- Oscillatory forces with the average force reflective of the sum of drag/potential energy forces related to the trailing units. The magnitude of oscillation is linked to road vertical profile.
- Large peaks due to low-speed shunting, such as take-off traction, braking or dithering between these. Whilst all units are braked, they are controlled by air pressure signal and as such there is a timing delay between application when the driver is modulating the towing unit brake.

Table 1 and Figure 7 below show a sample of results observed at speed, which are reflective of the first point above.

Table 2 and Figure 8 below show a sample of results observed at low speed (less than 10 km/h) and are reflective of the second point above. Across the datasets, low speed forces meet or exceed the maximum forces observed at speed.

Table 1 - At speed sample of measurements from associated Figure 7

Dolly position:	Front
Vehicle speed:	95.3 km/hr
Fifth wheel longitudinal force:	117.86 kN
Drawbar longitudinal force:	75.53 kN
Overturning moment:	-24.45 kNm
Scenario:	Typical road excitation (0.3G)
Occurrence:	Frequent

Table 2 - Low speed sample of measurements from associated Figure 8

Dolly position:	Front
Vehicle speed:	0 km/hr
Fifth wheel longitudinal force:	146.21 kN
Drawbar longitudinal force:	148.45 kN
Overturning moment:	-13.61 kNm
Scenario:	Acceleration from standstill
Occurrence:	Common during starting accelerations

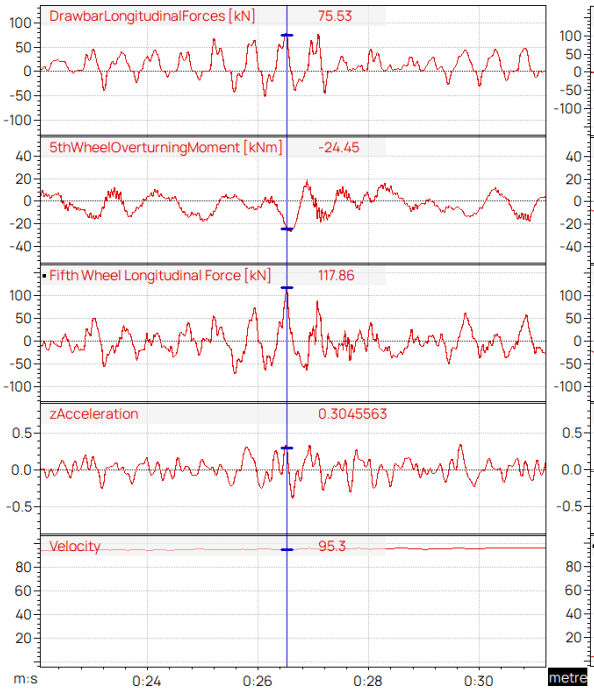

Figure 7 - At speed sample of force measurements

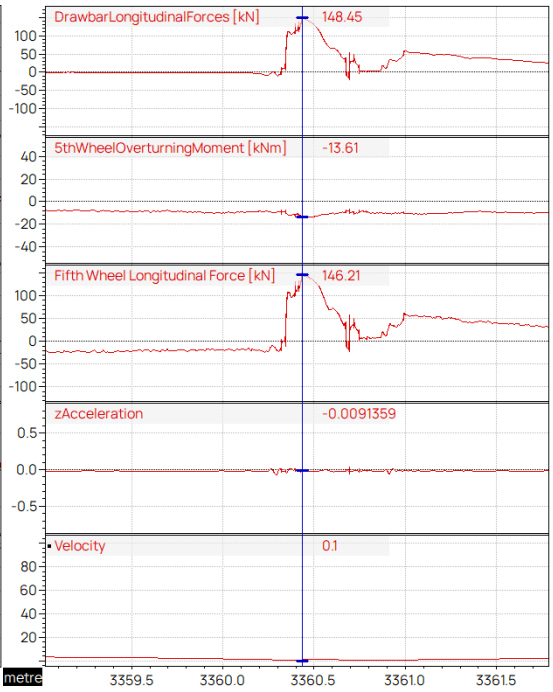

Figure 8 - Low speed sample of force measurements

Due to the a priori assumption that higher forces are more contributory to coupling lifetime damage, an algorithm was applied to the datasets to count how many instances of forces crossing a series of thresholds were incurred, whilst the combination was travelling at more than 10 km/h. This was then divided by the distance of the dataset, thereby normalising to events/1000 km. It should be noted that:

- Whilst identical routes were compared, speeds across features differ in some instances as a result of testing in real world conditions with traffic influence and unscheduled stops. The authors contend that the size of the input dataset minimises the influence of these factors.
- Long duration high force events were not witnessed, only transient peaks, so counting when a longitudinal force channel moves from below a threshold to above is offered as the most appropriate count of events rather than “samples above threshold” which can be influenced by double peaks. This is also more relevant to “fatigue life” where cyclical loading is more damaging than continuous equivalent loading.
- The bins are not exclusive, ie force events exceeding higher thresholds are included in the counts of lower thresholds, except where the measurement has oscillated

above and below a higher threshold without dropping below a lower one. This is how some higher thresholds can record larger counts than lower thresholds.

These comparisons are provided in Figure 9 and Figure 10.

Maximum thresholds exceeded are critical (horizontal axis), as is the frequency with which this occurs (vertical axis).

For each coupling type, the entire dataset available is compared here. Some unique features are present in each test, so a more direct comparison of controlled conditions is included in the complete report which is not yet published. The more direct comparison included the complete report is most appropriate to determine the relationship between mass before and after. No conclusions are drawn in this report due to its preliminary nature.

Very high magnitude forces were observed associated with combination "shunting" activities, which include braking, low speed dithering between acceleration and braking (ie crawling) and acceleration from a standstill. To quantify these, a count was also undertaken of how many instances were incurred of crossing force thresholds whilst travelling at less than 10 km/h. In this measurement however, as the datasets contained differing durations spent under 10 km/h, the normalisation is per 10 minute period at less than 10 km/h velocity. These comparisons are provided in Figure 11 and Figure 12.

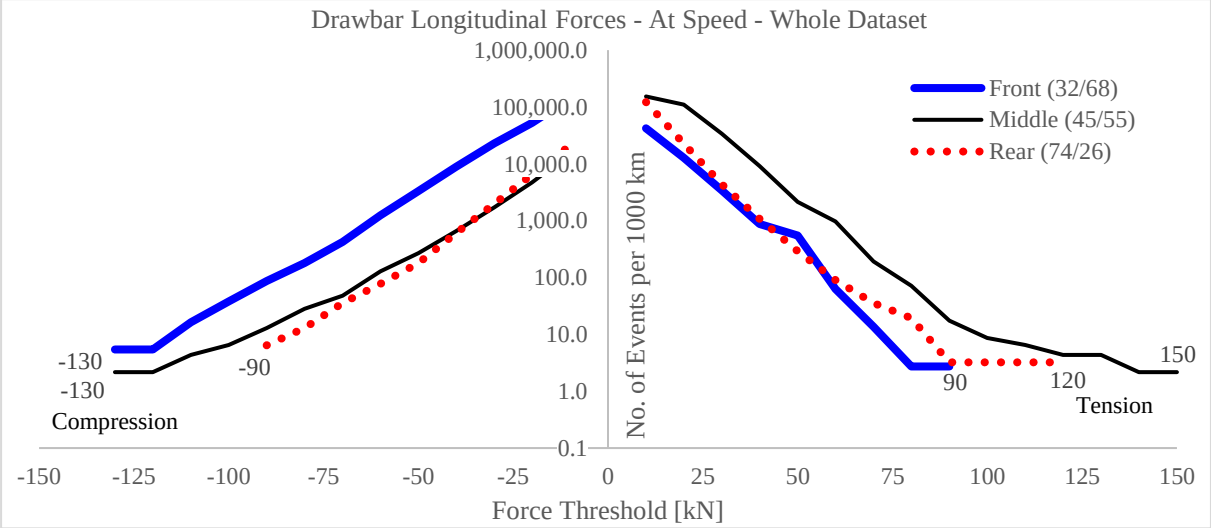

Figure 9 - Drawbar longitudinal forces at speed across the whole dataset

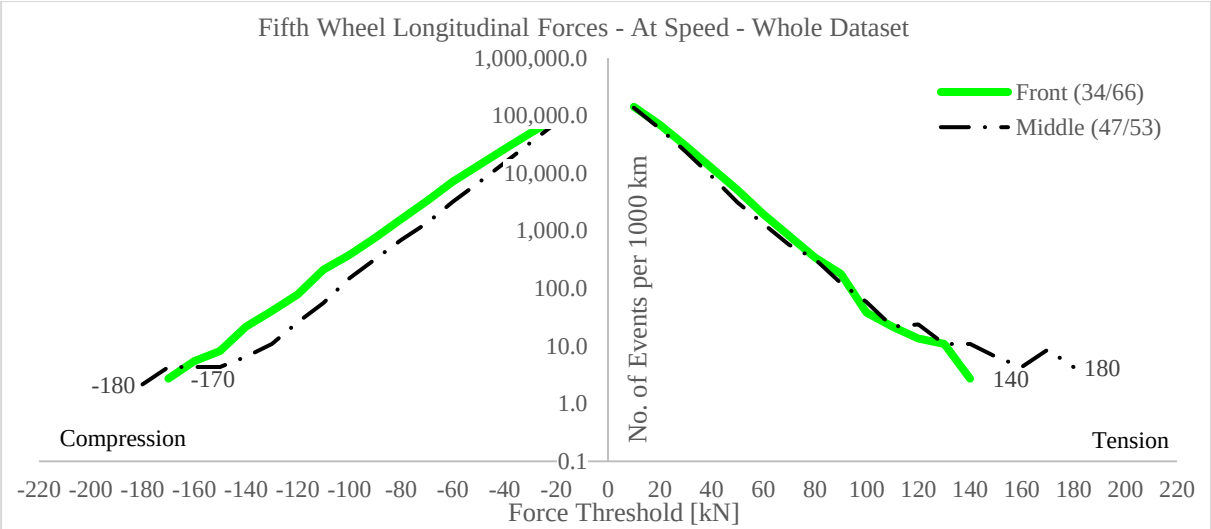

Figure 10 - Fifth wheel longitudinal forces at speed across the whole dataset

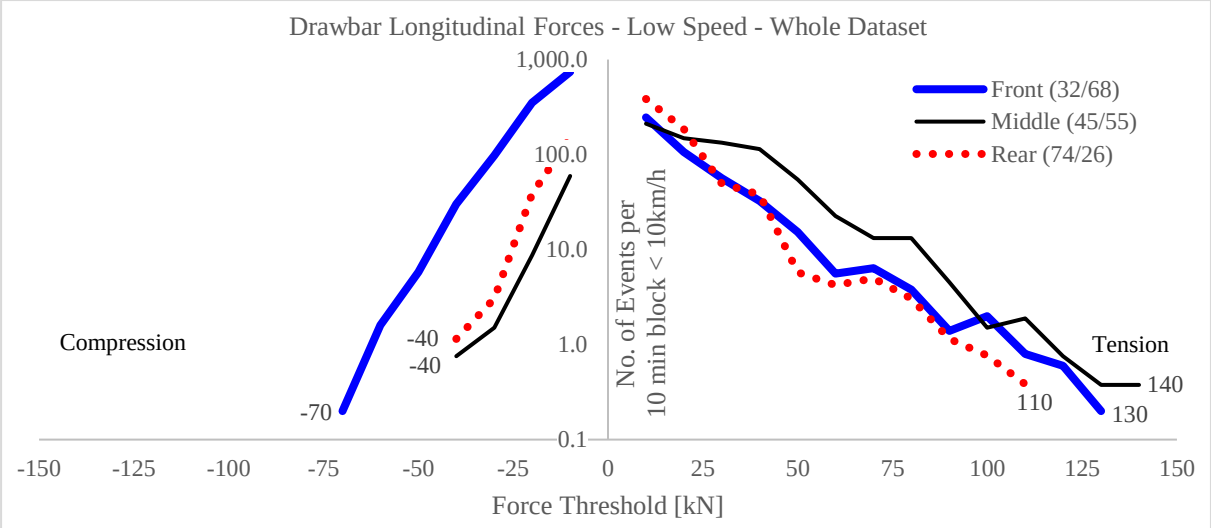

Figure 11 - Drawbar longitudinal forces at low speed across the whole dataset

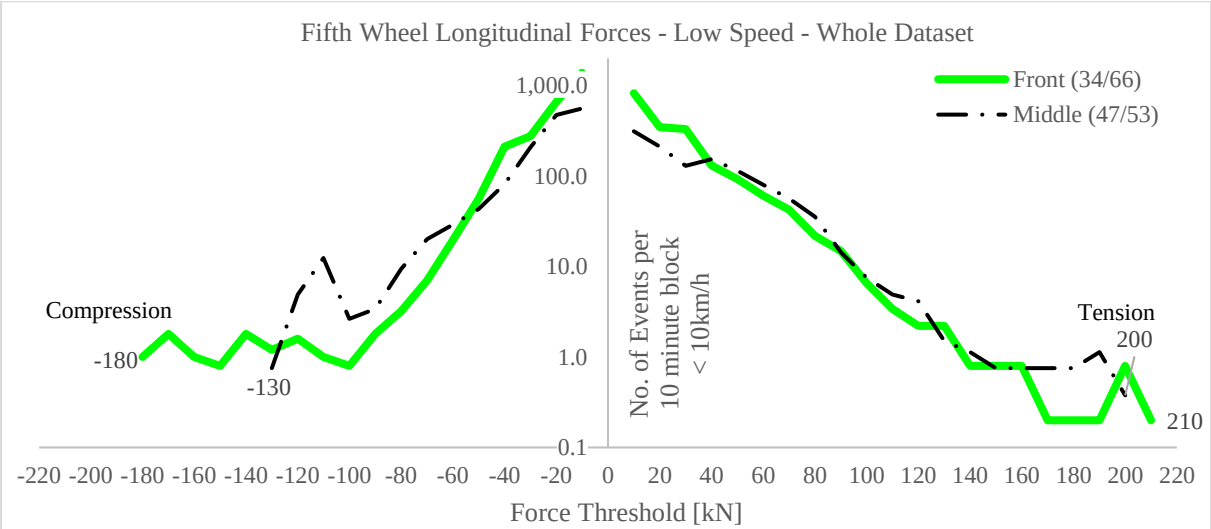

Figure 12 - Fifth wheel longitudinal forces at low speed across the whole dataset

4. Simulation Results

In order to expand the test program to other configurations of vehicle combinations, especially those which are presently uncommon or which would be impractical or unsafe to physically test, a program of simulation was additionally undertaken.

The tested vehicle was replicated in MSC Adams/Car. Correlation of the model consisted of adjusting the following parameters to match between simulated and physical results:

- Unit masses and axle group weights;
- Suspension geometry and parameters;
- Suspension damping to match the ratio of critical damping in a VSB11 Road Friendly Suspension test;
- Suspension parameters to match the natural frequency;
- Road profile, to match vertical sprung body accelerations; and,
- The amount of free lash and the spring rate of couplings.

This simulation is ongoing at the time of publication. An early sample is shown below in Figure 13.

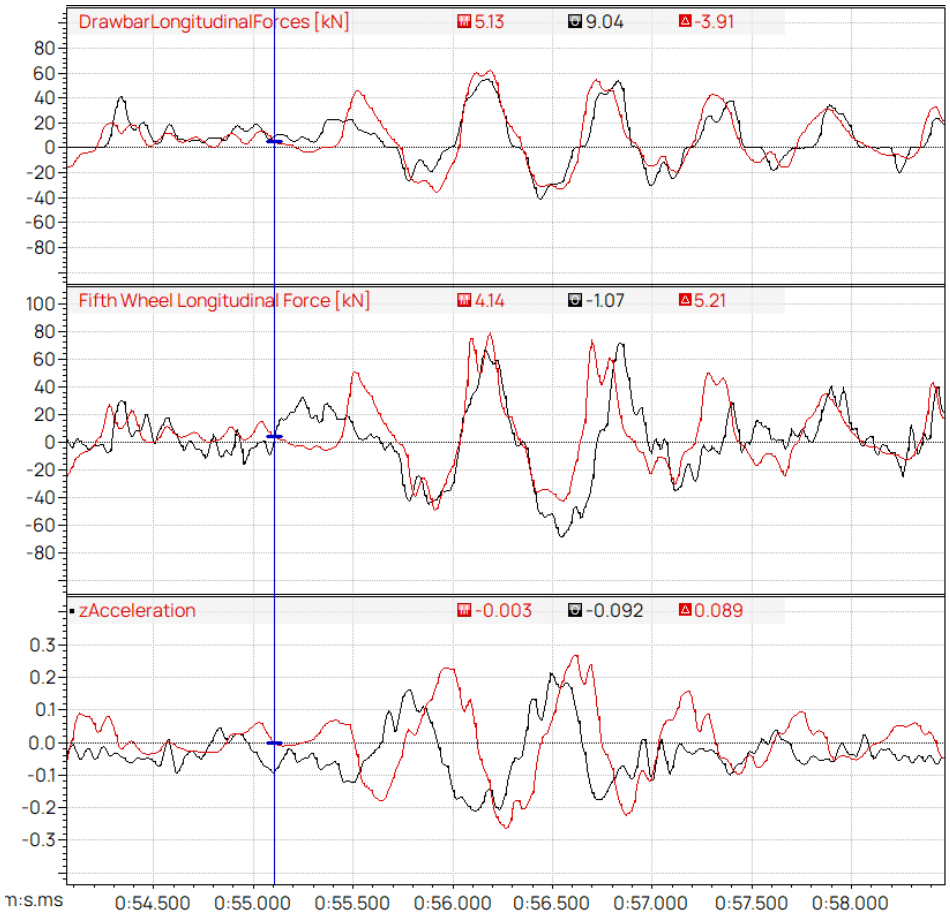

Figure 13 - Physical test data (black) compared with simulated data (red)

5. Conclusion

The results from the on-road testing show that the couplings may respond differently to what the equations in the AS2213.1 and AS4968.1 predict, specifically regarding the balance of mass before and after the coupling. No further conclusions are drawn for this publication, due to ongoing peer review.